Nuclear Instruments and Methods in Physics Research A 787 (2015) 6–11

Contents lists available at ScienceDirect

Nuclear Instruments and Methods in Physics Research A

journal homepage: www.elsevier.com/locate/nima

On the comparison of analog and digital SiPM readout in terms of expected timing performance

S. Gundacker*, E. Auffray, P. Jarron, T. Meyer, P. Lecoq

European Organization for Nuclear Research (CERN), 1211 Geneva 23, Switzerland

ARTICLE INFO

Available online 19 October 2014

Keywords:
Time of flight positron emission tomography (TOF-PET)
Coincidence time resolution (CTR)
Multi-digital SiPM
Analog SiPM
Maximum likelihood time estimator

ABSTRACT

In time of flight positron emission tomography (TOF-PET) and in particular for the EndoTOFPET-US Project (Frisch, 2013 [1]), and other applications for high energy physics, the multi-digital silicon photomultiplier (MD-SiPM) was recently proposed (Mandai and Charbon, 2012 [2]), in which the time of every single photoelectron is being recorded. If such a photodetector is coupled to a scintillator, the largest and most accurate timing information can be extracted from the cascade of the scintillation photons, and the most probable time of positron emission determined. The readout concept of the MD-SiPM is very different from that of the analog SiPM, where the individual photoelectrons are merely summed up and the output signal fed into the readout electronics. We have developed a comprehensive Monte Carlo (MC) simulation tool that describes the timing properties of the photodetector and electronics, the scintillation properties of the crystal and the light transfer within the crystal. In previous studies we have compared MC simulations with coincidence time resolution (CTR) measurements and found good agreement within less than 10% for crystals of different lengths (from 3 mm to 20 mm) coupled to SiPMs from Hamamatsu. In this work we will use the developed MC tool to directly compare the highest possible time resolution for both the analog and digital readout of SiPMs with different scintillator lengths. The presented studies reveal that the analog readout of SiPMs with microcell signal pile-up and leading edge discrimination can lead to nearly the same time resolution as compared to the maximum likelihood time estimation applied to MD-SiPMs. Consequently there is no real preference for either a digital or analog SiPM for the sake of achieving highest time resolution. However, the best CTR in the analog SiPM is observed for a rather small range of optimal threshold values, whereas the MD-SiPM provides stable CTR after roughly 20 registered photoelectron timestamps in the time estimator.

1. Introduction

Highest time resolution in scintillator-based detectors is becoming more and more important in applications for high energy physics and medical diagnostics [1]. Several commercial whole-body TOF-PET scanners have demonstrated that already ~500 ps in coincidence time resolution (FWHM) can give clear improvements in image signal to noise ratio (SNR) and contrast [3,4]. However, CTRs smaller than 100 ps FWHM are necessary to improve image SNR to the level that scanning times and radiation exposure to the patient can be significantly reduced. In PET, L(Y)SO crystals are commonly used to detect the 511 keV gammas and to produce scintillation photons to be sensed by photodetectors. Silicon photomultipliers (SiPMs) are promising candidates to achieve excellent time resolution [5–8]. In an analog SiPM signals from individual photon avalanche diodes (SPADs) are summed up, and the timing information is commonly derived from leading edge discrimination as can be seen in Fig. 1.

Another technique to detect the scintillation photons is to employ multi-digital SiPMs (MD-SiPMs) [2] as shown in Fig. 2. In these purely digital devices every photoelelectron detected in a SPAD is registered with its own timestamp, thus providing the maximum information of the scintillation photon rate. This idea was first commercialized by Philips [9]. However, it should be noted that the Philips device only has one TDC for a larger array of SPADs and is therefore essentially different from the MD-SiPM discussed in this work. In previous studies it was shown that the proper combination of all photoelectron timestamps obtained in the MD-SiPM noticeably improves the CTR [10–13]. However, the analog SiPM, with its characteristic leading edge discrimination, intrinsically performs such a combination as well, which is nothing but the average of the preceding photoelectron

* Corresponding author. Tel.: +41 22 767 4623.
E-mail address: stefan.gundacker@cern.ch (S. Gundacker).

http://dx.doi.org/10.1016/j.nima.2014.10.020

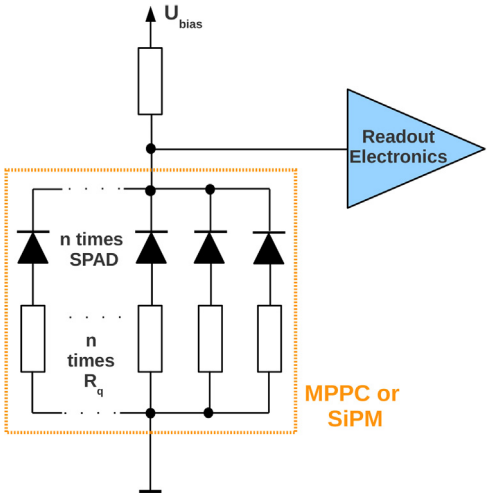

Fig. 1. In the analog SiPM the SPAD (microcell) signals are summed up and the positron emission time is estimated via leading edge discrimination.

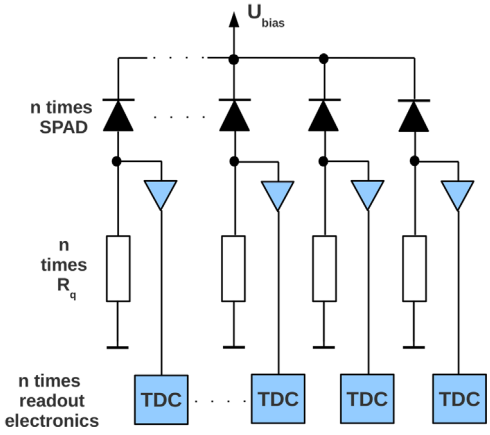

Fig. 2. In the multi-digital SiPM the timestamp of every photon detected is recorded with its own time to digital converter (TDC).

timestamps. It is therefore interesting to investigate and understand the inherent limitations in the highest possible time resolution for both the analog and digital readout of SiPMs. Because of the not yet available MD-SiPM measurements this is only possible within the framework of sophisticated Monte Carlo simulations.

\In this paper we will compare the analog and digital readout of SiPMs in terms of their expected timing performance in a TOF-PET system. After a detailed description of the positron emission time estimator derived in the analog SiPM we will introduce two different time estimators in the digital SiPM, i.e. a simple average of the gathered photoelectron timestamps and a maximum likelihood method taking into account the full covariance matrice of the system. Using our previously developed Monte Carlo (MC) tool [14] we are able to compare the best time resolution possible in a system employing an analog or a multi-digital readout of SiPMs. We follow with a discussion of the Cramér–Rao lower bound [11] of the time resolution and compare the calculated lower bound of the CTR with simulation results obtained for the analog and MD-SiPM.

2. Methods of estimating the positron emission time

2.1. Analog SiPM

In the analog SiPM a number of single photon avalanche diodes are connected in parallel, i.e. 3600 for the Hamamatsu S10931-050P MPPC. Each SPAD gives rise to a characteristic signal if an incident photon is being detected at time D_i. The SiPM output signal is the sum of all fired, single SPAD signals. If the SPAD signal is well described by a bi-exponential function with a rise time component of the order of a few 100 ps and a fall time component of several nanoseconds, then the overlap of the single SPAD signals will happen at the onset of the bi-exponential function. This assumption is justified on the grounds that a LSO scintillator gives a photon detection rate of typically 100 photoelectrons per nanosecond. Furthermore it should be noted that low pass filtering or bandwidth limitation of the electronics can enlarge the SPAD signal rise time value significantly. Within these limitations the SPAD signals can be approximated by a straight line, and the summed SiPM output signal is the sum of these linear slopes, as can be seen in Fig. 3 and as described in Eq. (1). The Heaviside function Θ ensures the SPAD signal to be zero before detection. The timestamp D_i denotes the time of the i-th photoelectron being detected and k is the gradient of the SPAD signals. The sum in Eq. (1) sums over all detected photoelectrons n':

$$V = \sum_{i=1}^{n'} k(t-D_i)\Theta(t-D_i). \tag{1}$$

The leading edge discrimination with a threshold value of V_{th}, performed by the analog readout, can be described by setting Eq. (1) equal to the threshold value V_{th} (see Eq. (2)). The resulting crossing time $\hat{\theta}_{analog}$ is the analog time estimator of the positron emission time as stated in Eq. (3):

$$V_{th} = \sum_{i=1}^{n_{V_{th}}} k(\hat{\theta}_{analog} - D_i)$$

$$V_{th} = n_{V_{th}} k\hat{\theta}_{analog} - \sum_{i=1}^{n_{V_{th}}} kD_i \tag{2}$$

$$\Rightarrow \hat{\theta}_{analog} = \frac{V_{th}}{n_{V_{th}} k} + \frac{1}{n_{V_{th}}} \sum_{i=1}^{n_{V_{th}}} D_i. \tag{3}$$

In Eq. (3) it can be seen that the analog SPAD signal pile-up with leading edge discrimination effectively is the average of the photoelectron timestamps. The term $n_{V_{th}}$ indicates that the number of photoelectrons averaged is dependent on the applied threshold V_{th}. The first term in Eq. (3) describes a constant offset, which is dependent on the number of photoelectrons averaged (threshold) and on the slope of the SPAD signal. It implies that a higher bias overvoltage and a higher number of detected photons lead to an earlier threshold crossing time. Because $n_{V_{th}}$ is a function of the photon emission rate and thus dependent on light yield fluctuations its variance is assumed to be not exactly zero.

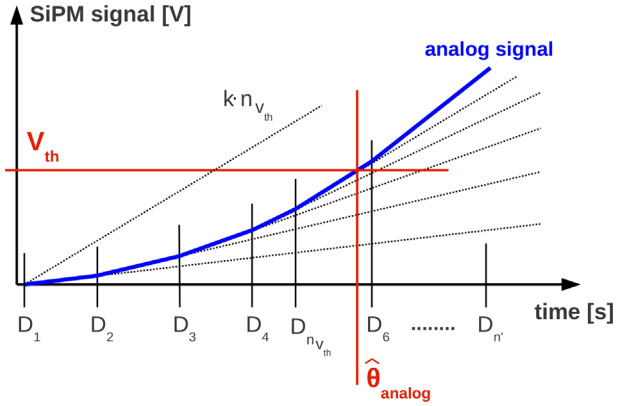

Fig. 3. The SPAD signal pile-up in the analog SiPM with leading edge discrimination leads to an effective average of the preceding photoelectron timestamps seen in the analog time estimator $\hat{\theta}_{analog}$. The time of each photoelectron detected is denoted as D_i with a total number of photoelectrons being detected n'.

2.2. Multi-digital SiPM

In the multi-digital SiPM the timestamp of every photoelectron detected (D_i) is being recorded. One possible time estimator would be to combine all timestamps D_i by taking the average. This approach will be referred to as "simple average" and is defined in Eq. (4) with $\widehat{\theta}_{sa}(K)$ describing the estimated time of positron annihilation for a given number K of averaged timestamps D_i. This approach is very close to the analog time estimator $\widehat{\theta}_{analog}$ in Eq. (3) and should give comparable CTR values:

$$\widehat{\theta}_{sa}(K) = \frac{1}{K}\sum_{i=1}^{K} D_i. \tag{4}$$

Another method is to obtain the most likely time of positron emission $\widehat{\theta}_{MLTE}$ via the maximization of the probability density function $P(\theta|\vec{D})$, which gives the probability of the positron emission time θ for a set of measured data $\vec{D}$ with length K. Using Bayes' theorem one can express $P(\theta|\vec{D})$ in terms of the likelihood function $P(\vec{D}|\theta)$ as shown in the following equation:

$$P(\theta|\vec{D}) = \frac{P(\theta)\cdot P(\vec{D}|\theta)}{P(\vec{D})}. \tag{5}$$

The term $P(\theta)$ in Eq. (5) denotes the prior which we define to be one, i.e. $P(\theta)=1$. This means that we assume no prior knowledge of the positron emission time and thus stay unbiased. We replace the likelihood function $P(\vec{D}|\theta)$ in terms of the multivariate normal distribution, see Eq. (6). This is justified as long as the photoelectron detection probability density functions can be approximated by a Gaussian. The denominator in Eq. (5) ($P(\vec{D})$) is a normalization factor independent on the positron emission time θ:

$$P(\vec{D}\,|\theta) = \frac{1}{\sqrt{(2\pi)^K|\mathbf{C}|}}\exp\left[-\frac{1}{2}\left(\vec{D}-\vec{\mu}-\vec{\mathbb{1}}\theta\right)^T\mathbf{C}^{-1}\left(\vec{D}-\vec{\mu}-\vec{\mathbb{1}}\theta\right)\right]. \tag{6}$$

The term $\mathbf{C}^{-1}$ in Eq. (6) denotes the inverse of the full covariance matrix and the elements of the vector $\vec{\mu}$ give the centroid of the i-th photon emissions. Both quantities can be obtained from an independent calibration run. The vector $\vec{\mathbb{1}}$ in Eq. (6) is the unity vector filled with ones and of length K. In order to obtain the most probable time of positron emission $\widehat{\theta}_{MLTE}$ we have to maximize the probability density function $P(\theta|\vec{D})$. The maximum can be found by setting its derivative to zero, i.e. $dP(\theta|\vec{D})/d\theta = 0$, as shown in Eq. (7). Because of the unity prior $P(\theta)=1$ the maximum of the probability density function $P(\theta|\vec{D})$ is equal to the minimum of the argument of the exponential of the likelihood function $\left[-0.5\left(\vec{D}-\vec{\mu}-\vec{\mathbb{1}}\theta\right)^T\mathbf{C}^{-1}\left(\vec{D}-\vec{\mu}-\vec{\mathbb{1}}\theta\right)\right]$:

$$\begin{aligned} 0 &= \frac{dP(\theta|\vec{D})}{d\theta} \\ 0 &= \frac{d}{d\theta}\left[-\frac{1}{2}\left(\vec{D}-\vec{\mu}-\vec{\mathbb{1}}\theta\right)^T\mathbf{C}^{-1}\left(\vec{D}-\vec{\mu}-\vec{\mathbb{1}}\theta\right)\right] \\ 0 &= \vec{\mathbb{1}}^T\mathbf{C}^{-1}\left(\vec{D}-\vec{\mu}-\vec{\mathbb{1}}\theta\right). \end{aligned} \tag{7}$$

In the last steps we applied the product rule and the transpose of the matrix multiplication $(\mathbf{AB})^T=\mathbf{B}^T\mathbf{A}^T$, together with the property of $\mathbf{C}$ being symmetric and thus $\mathbf{C}^{-1}$ being symmetric as well:

$$\Rightarrow \widehat{\theta}_{MLTE} = \frac{\vec{\mathbb{1}}^T\mathbf{C}^{-1}\left(\vec{D}-\vec{\mu}\right)}{\vec{\mathbb{1}}^T\mathbf{C}^{-1}\vec{\mathbb{1}}} = \vec{W}^T\left(\vec{D}-\vec{\mu}\right). \tag{8}$$

The time estimator for the most likely time of positron emission (see Eq. (8)) can as well be calculated from the generalized least squares method and was called Gauss–Markov estimator in the work of Venialgo et al. [12]. In the following discussions we will denote the time estimator $\widehat{\theta}_{MLTE}$ as the maximum likelihood time estimation (MLTE). It is interesting to note that the MLTE in Eq. (8) can be seen as a weighted average of the used K timestamps $D_1, D_2, \ldots, D_K$. Here the weighting factors are contained in the vector $\vec{W}$ with length K and are only dependent on the covariance $\mathbf{C}$, i.e. the system calibration.

3. Cramér–Rao lower bound

For the purpose of finding the best achievable time resolution we will use the Fisher information and the Cramér–Rao lower bound as discussed by Seifert et al. [11]. In statistics the Fisher information measures the information that the observable, random variable $\vec{D}$, carries about an unknown parameter θ in which the probability of $\vec{D}$ depends on. The inverse of the Fisher information describes the minimum variance of an unbiased estimator of the unknown parameter θ and is called the Cramér–Rao lower bound. In our case θ denotes the time of positron annihilation in the PET system, which we want to determine, and $\vec{D}$ describes the measured photon detection times of the cascade of scintillation photons gathered. Using the Cramér–Rao lower bound we can determine the minimum variance of θ under the assumption of a fully efficient estimator and thus the limit of the best time resolution possibly achievable. In Eq. (9) we state the simplified probability density function (PDF) of the scintillation photon emission rate with only one rise time constant (τ_r) and one fall time constant (τ_d):

$$\widehat{f}(t|\theta) = \frac{\exp\left(-\frac{t-\theta}{\tau_d}\right)-\exp\left(-\frac{t-\theta}{\tau_r}\right)}{\tau_d-\tau_r}\,\Theta(t-\theta). \tag{9}$$

Every photon detected by the SiPM undergoes a certain time smearing due to the transit time spread in the SiPM. This can be modeled by a Gaussian with the variance expressed by the single photon time resolution (SPTR) as shown in Eq. (10). It should be noted that this smearing could be extended to contain also the photon travel spread (PTS) in the crystal, however the shape would not be Gaussian anymore and thus we set the PTS to zero for simplicity. The parameter Δ_M expresses a possible electronic delay:

$$g(t) = \frac{1}{\sqrt{2\pi}\sigma_{SPTR}}\exp\left[-\frac{(t-\Delta_M)^2}{2(\sigma_{SPTR})^2}\right]. \tag{10}$$

The likelihood function of photon detection, given a certain gamma production time θ, can be expressed by Eq. (11). It is the convolution of the scintillation photon emission rate (see Eq. (9)) with the time smearing of the gamma detection system (SiPM photodetector) as can be seen in Eq. (10):

$$\widehat{f}_g(t|\theta) = \widehat{f}(t,\theta) * g(t) = \int_{-\infty}^{\infty}\widehat{f}(t'|\theta)g(t-t')\,dt'. \tag{11}$$

The convolution in Eq. (11) can be done (semi-) analytically, using the error-function with the following properties: $erf(\pm\infty) = \pm 1$ and $erf(0)=0$. The result is shown in the following equation:

$$\begin{aligned} \widehat{f}_g(t|\theta) = {} & \frac{1}{2(\tau_d-\tau_r)}\exp\left(\frac{2\tau_d(\Delta_M+\theta-t)+\sigma_{SPTR}^2}{2\tau_d^2}\right) \\ & \times\cdot\left(1-erf\left[\frac{\tau_d(\Delta_M+\theta-t)+\sigma_{SPTR}^2}{\sqrt{2}\sigma_{SPTR}\tau_d}\right]\right) \\ & +\frac{1}{2(\tau_d-\tau_r)}\exp\left(\frac{2\tau_r(\Delta_M+\theta-t)+\sigma_{SPTR}^2}{2\tau_r^2}\right) \end{aligned}$$

$$\cdot\left(1-erf\left[\frac{\tau_r(\Delta_M+\theta-t)+\sigma_{SPTR}^2}{\sqrt{2}\,\sigma_{SPTR}\,\tau_r}\right]\right) \quad (12)$$

In Eq. (12) the limit $\sigma_{SPTR}\to 0$ gives the scintillation photon emission rate $\widehat{f}(t|\theta)$, although shifted by Δ_M, which represents the electronic delay in Eq. (10).

The Fisher information $I(\theta)$ is the expectation value of the score $(\partial/\partial\theta)\log\widehat{f_g}(t|\theta)$ squared, as can be seen in Eq. (13) and being used in [11]:

$$I(\theta)=E\left[\left(\frac{\partial}{\partial\theta}\log\widehat{f_g}(t|\theta)\right)^2|\theta\right]=\int_{-\infty}^{\infty}\frac{1}{\widehat{f_g}(t|\theta)}\left(\frac{\partial\widehat{f_g}(t|\theta)}{\partial\theta}\right)^2 d\theta. \quad (13)$$

Supposing an unbiased estimator the Cramér–Rao lower bound can be expressed as the inverse of the Fisher information [11] (see Eq. (14)). If we suppose that the likelihood is independent and identically distributed (iid) for each of the photons, i.e. according to Eq. (12), then the Fisher information is additive [11]. In that case we can account for the integral number of photons detected $(n'=n\cdot PDE\cdot LTE)$ by adding the term n' in Eq. (14). Here n denotes the intrinsic light yield of the scintillator, PDE is the photon detection efficiency of the SiPM and LTE the light transfer efficiency in the crystal. The LTE gives the ratio between the photons arriving at the photodetector and the total amount of scintillation photons produced. The term $2\cdot\sqrt{2\cdot\ln(2)}\cdot\sqrt{2}=3.33$ converts to coincidence time resolution expressed in FWHM:

$$CTR_{LB}=3.33\cdot\sqrt{\frac{1}{n'\cdot I(\theta)}}. \quad (14)$$

Eq. (14) gives the best achievable coincidence time resolution possible for a given scintillation emission rate with a certain number of detected photoelectrons n' and SPTR of the photodetector. In the following section we will compare the CTR values obtained by the digital and analog Monte Carlo simulations with the lower bound of the time resolution.

4. Results

To compare the timing performance of the analog and the MD-SiPM we have used a previously developed, experimentally evaluated, Monte Carlo simulation tool [8]. The Monte Carlo simulations describe the whole detection chain of gamma ray conversion, scintillation light production and transport in the crystal, extraction and conversion in the SiPM and electronic readout, taking also into account the SPTR and electronic noise. The analog SiPM simulation results are in good agreement with measurements using SiPMs from Hamamatsu (S10931-050P MPPC) [14,8], to be seen in Figs. 4 and 5. Furthermore, our simulations are able to correctly estimate the CTR as a function of crystal length from 3 mm to 20 mm, which can be seen in Table 1. In Table 1 we also summarize the simulated influence of noise sources such as dark count, crosstalk and electronic noise. We notice that, within our simulations, these noise sources deteriorate the CTR by approximately 10 ps FWHM.

In order to test the different time estimators introduced in Section 2 we use this experimentally evaluated Monte Carlo simulation tool, but modified it to produce single timestamps for each detected photon, i.e. changing the readout strategy in the program. In the MD-SiPM every i-th detected photon is associated with a timestamp delay D_i, where i denotes the photon rank, which is the same in both arms of the coincidence setup. These timestamp delays D_i are used as input for the simple average $(\widehat{\theta}_{sa})$ and the MLTE $(\widehat{\theta}_{MLTE})$ time estimators in Eqs. (4) and (8), respectively. In this case the vector $\vec{\mu}$ in Eq. (8) becomes zero.

In Figs. 6 and 7 we show the results of the analog and digital simulations. The analog CTR is plotted as a function of the leading edge threshold V_{th} normalized to the single SPAD amplitude. Because of the finite SPAD signal rise time this value is not simply one to one correlated with the i-th photoelectrons detected (see Fig. 1). In the "digital CTR plots" the CTR of the single i-th timestamp (D_i) gives the variance converted to CTR of each single

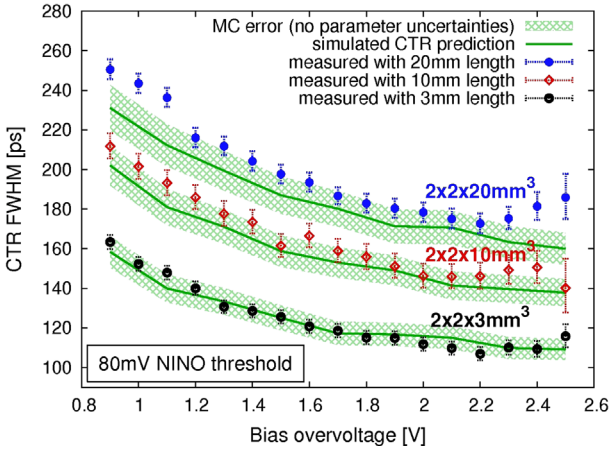

Fig. 4. Comparison of CTR simulations with measurements as a function of the SiPM bias overvoltage for crystals with dimensions of $2\times2\times3$ mm^3, $2\times2\times10$ mm^3 and $2\times2\times20$ mm^3 [8].

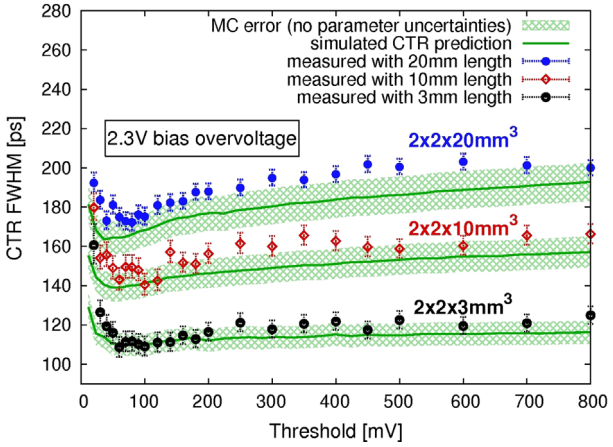

Fig. 5. Comparison of CTR simulations with measurements as a function of the NINO threshold voltage for crystals with dimensions of $2\times2\times3$ mm^3, $2\times2\times10$ mm^3 and $2\times2\times20$ mm^3 [8].

Table 1
Comparison of simulated and measured CTR in ps (FWHM) of an analog SiPM only (Hamamatsu S10931-050P) with and without noise sources such as dark count rate, crosstalk and electronic noise. For the measurements we used a LSO:Ce codoped 0.4%Ca crystal from the producer Agile. Always the best achieved CTR is compared. The simulation error is in the range of 5%, not including parameter uncertainties.

Crystal length (2×2 mm^2 cross-section)	**Measurement** (ps)	**Simulation** (ps)	
		With noise	Without noise
0 mm (LTE=0.68 and PTS=0)	–	90	82
3 mm (LTE=0.68)	108 ± 5	110	100
5 mm (LTE=0.62)	123 ± 7	121	111
10 mm (LTE=0.49)	143 ± 7	140	130
20 mm (LTE=0.39)	176 ± 7	166	152

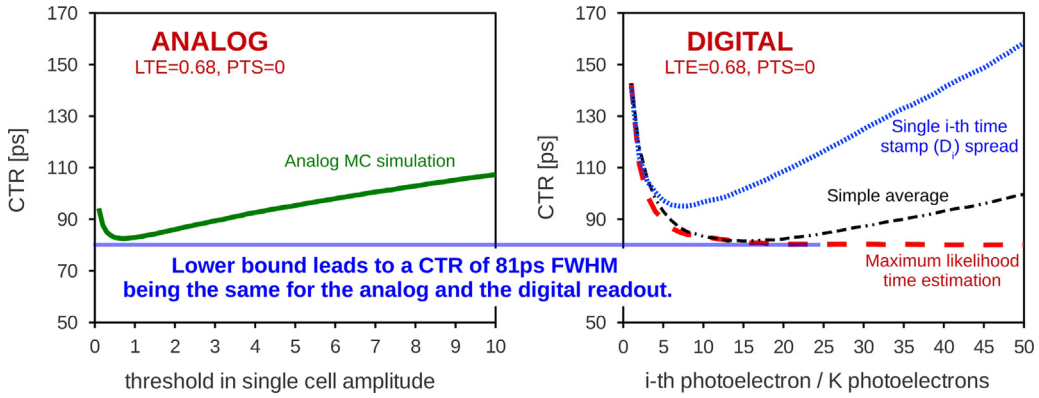

Fig. 6. Analog and MD-SiPM simulations for a hypothetical crystal with a light transfer efficiency of 68% (LTE=0.68 similar to the $2 \times 2 \times 3$ mm^3 case) and zero photon travel spread (PTS=0). In the simulations we set to zero the dark count rate and the crosstalk of the SiPM as well as the electronic noise. The simulation error is in the range of 5%, not including parameter uncertainties.

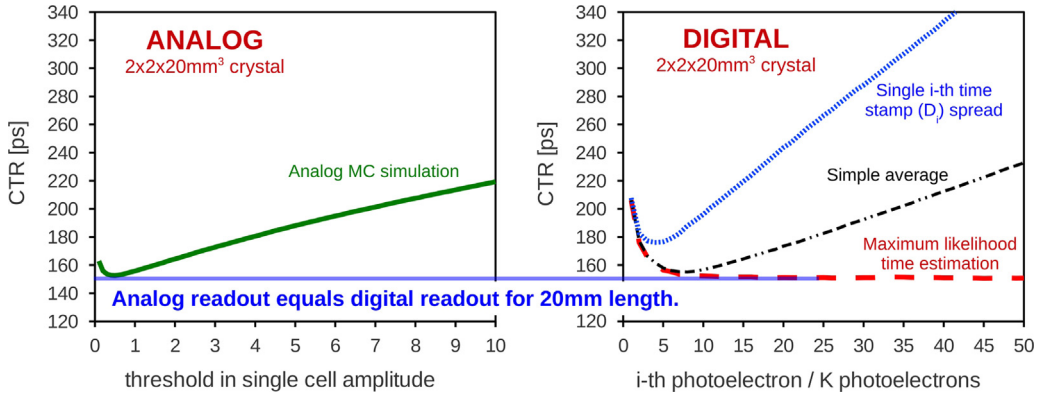

Fig. 7. Analog and MD-SiPM simulations for a crystal with dimensions of $2 \times 2 \times 20$ mm^3. In the simulations we set to zero the dark count rate and the crosstalk of the SiPM as well as the electronic noise. The simulation error is in the range of 5%, not including parameter uncertainties.

photon detected with rank i, i.e. without any combination of multiple timestamps. However, the simple average and maximum likelihood estimators combine the preceding timestamps up to rank K, at which the calculated CTR value is plotted according to Eqs. (4) and (8), respectively.

For the comparison of the different time estimators and SiPM types we chose the MC input parameters to be equal to our measurement results with LSO:Ce codoped 0.4%Ca scintillators with a rise time of $\tau_r = 70$ ps, a fall time of $\tau_d = 30.3$ ns and a total number of scintillation photons produced $n = 20\,400$ per 511 keV gamma [14]. The SPTR of the SiPM is set to 66 ps (sigma) and the photodetection efficiency (PDE) to 33%, identical for the digital and analog simulations. The shown simulations in Figs. 6 and 7 do not include optical crosstalk and the dark count rate (DCR) of the SiPM neither electronic noise of the readout electronics.

In Fig. 6 we show simulations with zero photon travel time spread in the crystal (PTS=0). Additionally, the light transfer efficiency was held constant at 68% (LTE=0.68) yielding a total number of 4577 photoelectrons detected per 511 keV gamma. The MC input parameters are chosen in such a way that we can compare the results with the Cramér–Rao lower bound introduced in the work of [11] and shown in Eq. (14), i.e. $\tau_r = 70$ ps, $\tau_d = 30.3$ ns, $n' = 4577$ and SPTR=66 ps. For the chosen parameters we calculate a lower bound of 81 ps FWHM CTR. With the simple average time estimator we obtain a CTR value of 82 ps, whereas the MLTE leads to a coincidence time resolution of 80 ps FWHM, as can be seen in Fig. 6. The statistical error of the simulated values is of the order of a few percent. This implies that both the simple average and the maximum likelihood time estimators in the MD-SiPM are able to reach the intrinsic limit of the time resolution derived from the Cramér–Rao lower bound. In Fig. 6 we also show the same MC simulations for the analog SiPM with SPAD signal pile-up. The best CTR value obtained at optimum threshold is 82 ps FWHM. Within the framework of our simulations it appears that both digital and analog readout are principally capable to reach the intrinsic limit of the time resolution. This is a direct consequence of the fact that the simple average time estimator shows almost the same performance as the more complex MLTE approach.

In Fig. 7 we depict MC simulations for the case of a $2 \times 2 \times 20$ mm^3 sized crystal. It can be seen that the digital readout

Table 2
Simulated CTR in ps (FWHM) of an analog and multi-digital SiPM as a function of crystal length *without* instrumental noise. Always the best achieved CTR is compared for the analog SiPM and the MD-SiPM with different time estimators. The simulation error is in the range of 5%, not including parameter uncertainties.

Crystal length (2×2 mm^2 cross-section)	**Analog SiPM** ($\widehat{\theta}_{analog}$) (ps)	**Multi-digital SiPM** (ps)		
		i-th time spread	Simple average ($\widehat{\theta}_{sa}$)	MLTE ($\widehat{\theta}_{MLTE}$)
0 mm (LTE=0.68 and PTS=0)	82	95	82	80
3 mm (LTE=0.68)	100	118	104	100
5 mm (LTE=0.62)	111	129	112	108
10 mm (LTE=0.49)	130	149	132	128
20 mm (LTE=0.39)	152	176	155	151

of the SiPM with the maximum likelihood time estimator gives CTR values that are comparable to the minimum CTR of an analog SiPM with its SPAD signal pile-up and leading edge discrimination.

In Table 2 we summarize the corresponding simulation results for both the analog SiPM and MD-SiPM readout. In the case of the digital readout we compare the different time estimators with the single i-th photoelectron time spread, i.e. the best CTR value obtained if no combination of the timestamps D_i is performed.

5. Conclusion

To investigate the multi-digital (MD) SiPM we have used an experimentally evaluated Monte Carlo simulation tool specially developed to describe the whole chain of gamma detection in a scintillator-based detector. In the case of the analog SiPM we used the pile-up of the single SPAD signals whereas in the MD-SiPM we modified the readout scheme of the MC tool to give the time information of every photoelectron detected. We compared two different time estimators in the digital SiPM, i.e. a simple average of the preceding detected photoelectrons and a more sophisticated maximum likelihood time estimation (MLTE). Our analysis shows that the analog and digital readout of SiPMs can lead to very similar timing performances for LSO type crystals. This is a direct consequence of the comparable performance of the simple average and maximum likelihood time estimation in the MD-SiPM. However, best CTR values in the analog SiPM (and for the simple average time estimation) are observed for a rather small range of optimal threshold values (averaged timestamps), whereas the multi-digital SiPM with MLTE provides stable CTR after roughly 20 registered photoelectron timestamps. This could render the MD-SiPM more robust against electronic and detector noise. In further work we will engage in studies with different crosstalk models for the analog and digital SiPM and their impact on the highest achievable time resolution.

Acknowledgments

We wish to thank Alain Machard for building the dark boxes of our experimental setups and Dominique Deyrail for preparing the crystals. This work was carried out in the frame of the Crystal Clear Collaboration, the EndoTOFPET-US Project (European Union Seventh Framework Program under Grant agreement n256984, Health-2010.1.2-1) and the TICAL ERC Grant 338933.

References

[1] B. Frisch, Nuclear Instruments and Methods in Physics Research Section A 732 (2013) 577, On behalf of the EndoTOFPET-US Collaboration.
[2] S. Mandai, E. Charbon, Multi-channel digital SiPMs: concept, analysis and implementation, in: Nuclear Science Symposium and Medical Imaging Conference Record (NSS/MIC), N34-4, 2012, pp. 1840–1844.
[3] J.S. Karp, S. Surti, M.E. Daube-Witherspoon, G. Muehllehner, Journal of Nuclear Medicine 49 (3) (2008) 462.
[4] S. Surti, A. Kuhn, M.E. Werner, A.E. Perkins, J. Kolthammer, J.S. Karp, Journal of Nuclear Medicine 48 (March) (2007) 471.
[5] C. Kim, G. Wang, S. Dolinsky, IEEE Transactions on Nuclear Science NS-56 (October) (2009) 2580.
[6] R. Vinke, H. Löhner, D. Schaart, H. van Dam, S. Seifert, F. Beekman, P. Dendooven, Nuclear Instruments and Methods in Physics Research Section A 610 (2009) 188.
[7] J.Y. Yeom, R. Vinke, C.S. Levin, Physics in Medicine and Biology 58 (2013) 1207.
[8] S. Gundacker, A. Knapitsch, E. Auffray, P. Jarron, T. Meyer, P. Lecoq, Nuclear Instruments and Methods in Physics Research Section A 737 (February) (2014) 92.
[9] T. Frach, G. Prescher, C. Degenhardt, R. Gruyter, A. Schmitz, R. Ballizany, IEEE Nuclear Science Symposium Conference (2009) 1959.
[10] M.W. Fishburn, E. Charbon, IEEE Transactions on Nuclear Science NS-57 (October) (2010).
[11] S. Seifert, H.T. vanDam, D.R. Schaart, Physics in Medicine and Biology 57 (2012) 1797.
[12] E. Venialgo, S. Mandai, E. Charbon, Time mark estimators for MD-SiPM and impact of system parameters, in: Nuclear Science Symposium Conference record (NSS/MIC), November 2013.
[13] S. Gundacker, Time resolution in scintillator based detectors for positron emission tomography (Ph.D. thesis), Vienna University of Technology, 2014.
[14] S. Gundacker, E. Auffray, B. Frisch, P. Jarron, A. Knapitsch, T. Meyer, M. Pizzichemi, P. Lecoq, Journal of Instrumentation 8 (August) (2013) P07014.